Smart Hydrogel Grating Immunosensors for Highly Selective and Sensitive Detection of Human-IgG

Jia-Jia Zhao,[†] Wei Wang,[,†,‡] Fang Wang,[†] Yu Zhao,[†] Quan-Wei Cai,[†] Rui Xie,[†,‡] Xiao-Jie Ju,[†,‡] Zhuang Liu,[†,‡] Yousef Faraj,[†,‡] and Liang-Yin Chu,[*,†]*

[†]School of Chemical Engineering, Sichuan University, Chengdu, Sichuan 610065, China

[‡]State Key Laboratory of Polymer Materials Engineering, Sichuan University, Chengdu, Sichuan 610065, China

ABSTRACT:

A smart diffraction grating immunosensor based on antigen-responsive hydrogel with enhanced analyte-induced volume changes is developed for highly selective and sensitive detection of human immunoglobulin G (H-IgG). The hydrogel grating contains poly(*N*-isopropylacrylamide) (PNIPAM) backbones with dual-crosslinking based on the dynamic complexation between pendent goat-anti-human IgG (GAH-IgG) and pendent H-IgG, and the covalent bonding by 4-arm-polyethylene glycol-acrylamide. Upon recognizing free H-IgG in the environment, the pendent GAH-IgG in the hydrogel can form new GAH-IgG/H-IgG complexes with free H-IgG because the binding constant of GAH-IgG to the free H-IgG is much larger than that to the pendent H-IgG, and thus result in the decomplexation of GAH-IgG/H-IgG complexes with the pendent H-IgG as well as the swelling of hydrogel. The thermo-responsive PNIPAM backbones enable enhancement of H-IgG-responsive volume change of the proposed hydrogel grating via temperature regulation. Moreover, the crosslinker 4-arm-polyethylene glycol-acrylamide provides excellent transparency for the PNIPAM backbones during the volume change, which ensures to output diffracted optical signals with high intensity. With the elaborately designed molecular structures, the hydrogel grating allows highly selective and sensitive detection of [H-IgG] with detection limit as low as of 1.3×10^{-8} M. This work provides a simple and flexible strategy for developing diffraction grating immunosensors based on stimuli-responsive hydrogels for efficient detection of biomarkers.

KEYWORDS:

Immunosensors; Diffraction gratings; Human-IgG; Smart hydrogels; Antigen

INTRODUCTION

Detection of biomarkers is crucial for early diagnosis of diseases, assessment of disease severity, and reflection of drug effects and pharmacokinetics.[1-4] Especially, human immunoglobulin G (H-IgG) is one of the important biomarkers that can indicate diseases such as primary or secondary immunodeficiency, and infection diseases,[5-8] which makes the detection of H-IgG highly important in clinical diagnostics. Typically, detection of immunoglobulin G can be achieved by using electrochemical methods,[9,10] quartz crystal microbalances,[11,12] surface plasmon resonance,[13,14] enzyme-linked immunosorbent assay[15] and chemiluminescent methods.[16] As compared to the conventional detection methods, diffraction grating sensors provide an efficient and versatile approach for biomarker detection, due to their advantages such as low cost, easy operation, and high sensitivity and flexibility.[17-22] Usually, the detections with diffraction grating sensors require analyte-induced structural changes of the diffraction gratings to regulate the diffracted optical signals as readouts. Thus, high-performance detection by the diffraction grating sensors usually requires the grating materials with significant structural changes that are highly selective and sensitive to the target analytes. Smart hydrogels that can change their physical/chemical properties in response to specific stimuli, are promising candidates for satisfying the above-mentioned requirements. Therefore, development of diffraction grating sensors from smart hydrogels show great power for highly selective and sensitive detection of H-IgG.

Typically, hydrogel grating sensors can transduce the analyte signals via analyte-induced structural changes into changes of diffracted optical signals including the distance between the zero-order and first-order diffraction spots,[23] refractive index (*RI*),[24] and diffraction efficiency (*DE*)[21,22,25-27] for detection. For example, the

analyte-induced volume changes can vary the height and width of hydrogel gratings, leading to changes of distances between the zero-order and first-order diffraction spots.[23] However, the manual measurement of such distance changes usually results in limited accuracy for sensitive detection. More sensitive detection can be achieved by using optical instruments such as camera[28] and photodiodes[29] with image/data processing software for measuring the *RI* and *DE* changes. For example, when fixed on a substrate, the hydrogel grating allows only height change from the analyte-induced volume change, which can lead to the change of *RI* for sensitive detection by using photosensors.[24] As compared to the above-mentioned detections, the detection based on *DE* changes is more widely used for detecting various analytes.[30-42] For example, the height change of hydrogel grating fixed on substrate can also lead to the zero-order and first-order diffraction spots with fixed positions. This allows use of two fixed photodiodes to accurately detect the intensities of these zero-order and first-order beams for analyzing the *DE* changes for sensitive detection. Such a detection strategy based on *DE* changes has been used to detect a wide range of analytes including DNA,[30,31] amino acid,[32] proteins,[33-35] volatile substances,[36,37] and low molecular weight organic compounds.[26] However, although hydrogel gratings based on *DE* measurement have also been developed for detection of H-IgG,[38] their intrinsic molecular structures restrict the volume change at low H-IgG concentration ([H-IgG]), resulting in limited sensitivity. Therefore, development of smart hydrogel grating immunosensors with high selectivity and sensitivity for efficient detection of H-IgG is still highly desired.

Here we report on smart diffraction grating immunosensors based on antigen-responsive hydrogels with enhanced analyte-induced volume changes for highly selective and sensitive detection of H-IgG. The hydrogel grating contains

poly(*N*-isopropylacrylamide) (PNIPAM) backbones that are dynamically crosslinked via reversible complexation between the pendent goat-anti-human IgG (GAH-IgG) and pendent H-IgG, and covalently crosslinked via 4-arm-polyethylene glycol-acrylamide (tetra-arm star PEGAAm). The pendent GAH-IgG units in GAH-IgG/H-IgG complexes can specifically recognize free H-IgG in the sample solution because the binding constant of GAH-IgG to free H-IgG is much larger than that to the pendent and denatured H-IgG, and lead to decomplexation of GAH-IgG/H-IgG complex as well as the swelling of hydrogel grating. The PNIPAM backbones with thermo-responsive volume changes enable enhancement of the H-IgG-induced swelling via temperature regulation. Meanwhile, with tetra-arm star PEGAAm as crosslinker,[39] PNIPAM backbones can preserve excellent transparency during their volume changes, to maintain high intensity for the diffracted optical signal. With elaborately designed molecular structures for synergistic integration of the above-mentioned features, the hydrogel grating allows enhanced [H-IgG]-dependent swelling to output a significant diffraction signal. The diffraction signal can be easily detected by a simple optical detection system. With the proposed smart hydrogel grating immunosensor, highly selective and sensitive detection of trace H-IgG can be easily achieved with a detection limit as low as 1.3×10^{-8} M.

EXPERIMENTAL SECTION

Materials. H-IgG, dog-IgG, goat-IgG, bovine-IgG, and pig-IgG, and GAH-IgG were purchased from Solarbio Life Science. *N*-isopropylacrylamide (NIPAM) and acrylamide (AAm) were purchased from TCI. NIPAM was purified by recrystallization with a hexane/acetone mixture. Tetra-arm star PEGAAm was

purchased from Ponsure Biotechnology. 3-acryloxypropyl trimethoxysilane was purchased from Beijing Bailingwei Chemicals. *N*-acryloxysuccinimide was purchased from Macklin. *N,N,N′,N′*-tetramethyl-ethylenediamine (TEMED), ammonium persulphate, sodium chloride, dibasic sodium phosphate, and sodium dihydrogen phosphate were purchased from Chengdu Kelong Chemicals. Pure water (18.2 MΩ at 25 ºC) from a Milli-Q Plus water purification system (Millipore) was used for all the experiments.

Silanization of Glass Slide with (3-Acryloxypropyl) Trimethoxysilane. The glass slide was silanized according to the method reported in published literatures.[40,41] First, the acetic acid/sodium acetate buffer (pH=5) containing 1 vol% 3-acryloxypropyl trichlorosilane was continuously stirred for 30 min for hydrolysis. Then, the glass slide was immersed in this buffer solution for 10 min for silanization. Next, the silanized glass slide was placed in an oven at 60 °C for 10 min. After that, the silanized glass slide was rinsed with deionized water, and dried for further use.

Preparation of Antigen-Responsive Hydrogel Gratings. The antigen-responsive hydrogel gratings were fabricated on the silanized glass slides via microcontact printing technology (Figure 1a). First, H-IgG (1.5 mg) was coupled with *N*-acryloxysuccinimide (0.1 mg) in phosphate buffer solution (PBS) (1000 μL, pH=7.4) at 36 ºC for 1 h via conjugation reaction to form vinyl-modified H-IgG, and then retreated with affinity chromatography (HiTrapTM, 1 mL) for purification. Similarly, same procedure was conducted by using GAH-IgG (0.75 mg) and *N*-acryloxysuccinimide (0.1 mg) to form vinyl-modified GAH-IgG. For fabrication of the antigen-responsive hydrogel grating, PBS (400 μL, pH=7.4) containing the vinyl-modified H-IgG (1.1 mg) and GAH-IgG (0.59 mg), monomers NIPAM (72 mg) and AAm (11 mg), biocompatible crosslinker tetra-arm star PEGAAm (16 mg) and

ammonium persulphate (1 mg) was used as precursor solution. After adding TEMED (10 μL) into the precursor solution, a drop of the precursor solution (8 μL) was quickly added onto the surface of silanized glass slide. Then, a stamp of polyethylene terephthalate (PET), with size of 20 mm × 10 mm, was immediately placed onto the precursor solution on the silanized glass slide. Next, the precursor solution sandwiched between the PET stamp and the silanized glass slide was placed at 5 ^{o}C for 6 h for polymerization. Finally, the antigen-responsive hydrogel grating was created on the silanized glass substrate after removing the PET stamp and washing with PBS for many times to ensure the removal of residual chemicals.

Morphological and Structural Characterizations of Antigen-Responsive Hydrogel Gratings. The morphology and microstructure of antigen-responsive hydrogel gratings were observed using scanning electron microscope (SEM, TM3030, Hitachi) and atomic force microscopy (AFM, MultiMode 8, Bruker).

Setup of Optical Detection Platform based on Hydrogel Grating. For detection of H-IgG, an optical detection platform was constructed based on the antigen-responsive hydrogel grating (Figure 1b). A diode laser beam (LDM635, Thorlabs) was used as the light source for the detection. The hydrogel grating on the glass slide was immersed vertically in a 10 mL quartz cell, with the laser beam perpendicularly irradiating through the hydrogel grating. The quartz cell contains sample solution with H-IgG, with temperature controlled by a heating stage (RTL 110/B, Shanghai hotz). The intensities of the first-order (I_1) and zero-order (I_0) beams diffracted through the hydrogel grating were detected by using two silicon photodiodes (DSi200, Zolix) fixed on an optical stage (OTBP812-100-1, Zolix). The detected signals were collected and amplified by using data acquisition system (DCS300PA, Zolix) for analysis.

Study on Temperature- and [H-IgG]-Responsive Volume Changes of Hydrogel Grating. The effect of temperature on the volume change of hydrogel grating was investigated by incubating the hydrogel grating in aqueous solutions at different temperatures. The height (h) and width (w) of hydrogel grating in the solution at each temperature were measured by using AFM. Before each measurement, the hydrogel grating had been equilibrated for 20 min after adding the aqueous solution. Similarly, the effect of [H-IgG] on the volume change of hydrogel grating was investigated by incubating the hydrogel grating in aqueous solutions with different [H-IgG] values at a fixed temperature.

Detection of H-IgG with Hydrogel Grating Immunosensors. The performances of hydrogel grating immunosensors for detection of H-IgG were studied by using sample solutions with different concentrations of H-IgG. The signals of I_1 and I_0 were detected by the silicon photodiodes after the equilibrated swelling of hydrogel gratings in sample solutions at a fixed temperature. The first-order diffraction efficiency, defined as $DE=I_1/I_0$, was used to evaluate the [H-IgG] value. Similarly, the selectivity of hydrogel grating immunosensors for detection of H-IgG was investigated by using aqueous solutions with different antigens. Dog-IgG, goat-IgG, bovine-IgG, and pig-IgG, each with concentration of 4×10^{-7} M, was respectively used as the control group. Moreover, the H-IgG concentrations in real serum samples after diluted by PBS (pH=7.4, 0.1 M) are detected using the hydrogel grating immunosensors. The detection results are compared with those detected by commercialized available enzyme-linked immunosorbent assay (ELISA) method.

RESULTS AND DISCUSSION

Design of Molecular Structure of Antigen-Responsive Hydrogel Grating

Immunosensors for Detection of H-IgG. For highly selective and sensitive detection of H-IgG, the molecular structure of hydrogel grating is elaborately designed by using dual-crosslinking strategy. The PNIPAM backbones of the hydrogel grating are dynamically crosslinked via reversible GAH-IgG/H-IgG complexes, and covalently crosslinked by tetra-arm star PEGAAm. The crosslinked PNIPAM backbones work as actuators to achieve volume changes, while the pendent GAH-IgG units in GAH-IgG/H-IgG complexes serve as sensors to achieve highly selective recognition of free H-IgG. Upon recognizing the free H-IgG in the environment, the pendent GAH-IgG units can form new complexes with free H-IgG due to the decomplexation of GAH-IgG/H-IgG complexes with the pendent H-IgG (Figure 1c), because the binding constant of GAH-IgG to free H-IgG is much larger than that to the pendent and denatured H-IgG.[42] Due to the decomplexation of the pendent GAH-IgG/H-IgG complexes, the hydrogel grating swells and leads to changes of the *DE* value (Figure 1c). Since the volume swelling is resulted from accumulated changes based on the decomplexation of the pendent GAH-IgG/H-IgG complexes, the volume change of hydrogel grating is directly related to the [H-IgG] value. Meanwhile, the PNIPAM backbones crosslinked by tetra-arm star PEGAAm enable high transparency during volume changes to ensure a high intensity for the diffracted optical signal. Moreover, since PNIPAM-based hydrogels usually can exhibit different volume change behaviors depending on temperature,[43,44] the PNIPAM backbones provide an opportunity to further enhance the H-IgG-induced swelling of the hydrogel grating by regulating the operation temperature. Thus, with the proposed molecular structure, the hydrogel grating can transduce the [H-IgG] signals into significant diffracted optical signals via the enhanced [H-IgG]-dependent volume changes. The volume swelling of the hydrogel grating mainly leads to the

variation of I_1 value, as well as the *DE* value. To evaluate the detection performances of hydrogel grating immunosensors, a parameter (R_{DE}) is defined as $R_{DE}=(DE_{T,0}-DE_T)/DE_{T,0}$, in which $DE_{T,0}$ and DE_T are respectively the *DE* values for the hydrogel grating in solutions without H-IgG and with H-IgG at temperature *T*.

Fabrication of Antigen-Responsive Hydrogel Grating Immunosensors. To synthesize the antigen-responsive hydrogel gratings, a precursor solution containing the vinyl-modified H-IgG and GAH-IgG, monomers NIPAM and AAm, crosslinker tetra-arm star PEGAAm, and initiator ammonium persulphate is used. After polymerization of the precursor solution templated by the PET stamp, the antigen-responsive hydrogel grating is fabricated on the silanized glass slide via microcontact printing technology. UV analyses of the washing solutions (Figure S1) from affinity chromatography confirm no presence of vinyl-modified H-IgG and vinyl-modified GAH-IgG in the washing solution, indicating the successful polymerization of the designed hydrogel gratings.

The optical image of the prepared antigen-responsive hydrogel grating on a glass slide presents a clear diffraction phenomenon (Figure 2a). The uniform and periodic surface relief structures of the hydrogel gratings are confirmed by the SEM image and AFM images (Figure 2b-f). The dried hydrogel grating is featured with w=1.78 μm and h=31 nm (Figure 2c,d), while the hydrated hydrogel grating is featured with w=1.78 μm and h=234 nm (Figure 2e,f). Although the h value increases from 31 nm to 234 nm when the hydrogel grating changes from dried state to hydrated state, the widths of both dried and hydrated hydrogel gratings remains unchanged, due to the fixation of hydrogel grating on the silanized glass slide.

Effects of Temperature and [H-IgG] on the Volume Changes of Hydrogel Grating Immunosensors. Due to the thermo-responsive property of the

PNIPAM-based backbones, the hydrogel grating enables temperature-responsive volume changes. Since the hydrogel grating is fixed on the glass slide, such a volume change only leads to changes of the *h* value (Figures 3 and S2). When the temperature increases from 25 ºC to 50 ºC, the *h* value of hydrogel grating decreases dramatically from 234 nm to 127 nm (Figure 3a), while the *w* value remains nearly unchanged (Figure 3b).

With pendent GAH-IgG and pendent H-IgG incorporated in the PNIPAM backbones, volume changes of hydrogel gratings can also be isothermally induced by recognizing free H-IgG in the environmental solutions. Figure 4 summarizes the [H-IgG]-responsive size changes of hydrogel grating in sample solutions with different [H-IgG] values at 25 ºC. With increasing the [H-IgG] value from 0 M to 5.3×10^{-7} M, the *h* value of hydrogel grating increases linearly from 234 nm to 263 nm (Figure 4a), while the *w* value of hydrogel grating remains nearly unchanged (Figure 4b). The linear relationship between the *h* value and the [H-IgG] value ensures the good performance of hydrogel grating for detection of H-IgG based on the [H-IgG]-responsive volume changes. Meanwhile, the detection sensitivity of hydrogel gratings mainly depends on their height and width changes in response to [H-IgG]. For the hydrogel grating with fixed width, the value of *DE* is proportional to the square of the hydrogel grating height.[21] Thus, the large [H-IgG]-dependent *h* changes of hydrogel grating enable generation of significant diffraction signals for sensitive detection.

Moreover, as compared to normal PNIPAM-based hydrogel that becomes opaque upon shrinking,[45,46] the proposed hydrogel grating can remain good transparency upon volume changes. When the temperature increases from 20 ºC to 50 ºC, although the prepared hydrogel grating dramatically shrinks (Figure 3a), the shrunken hydrogel

grating can still exhibit excellent transparency with transmittance as high as ~98 % (Figure S3). The excellent transparency of hydrogel grating during the volume change is due to the introduction of tetra-arm star PEGAAm as crosslinker. The tetra-arm star PEGAAm can reduce the aggregation of hydrophobic side chains of PNIPAM backbones, and thus improve the transparency of shrunken hydrogel grating.[39] Such an excellent transparency of the hydrogel grating allows high intensity of the diffracted optical signals for achieving efficient detection of H-IgG.

Highly Selective Detection of H-IgG with Hydrogel Grating Immunosensors. High selectivity is one of the most important advantages for use of biological molecules as the recognition elements of biosensors. In our hydrogel grating, the use of specific antigen-antibody interaction ensures the high selectivity to H-IgG. To confirm the high selectivity, different antigens including dog-IgG, goat-IgG, bovine-IgG and pig-IgG, each with the same concentration as that of H-IgG (4×10^{-7} M), are used as control groups. For all the solutions respectively containing dog-IgG, goat-IgG, bovine-IgG and pig-IgG, the hydrogel gratings show very low R_{DE} values less than 0.03 (Figure 5). However, for the solution containing H-IgG (4×10^{-7} M), the hydrogel grating shows a R_{DE} value as high as 0.16. The results confirm the high selectivity of our hydrogel grating immunosensors based on the specific antigen-antibody interaction for detecting H-IgG.

Highly Sensitive Detection of H-IgG with Hydrogel Grating Immunosensors. Due to the [H-IgG]-responsive volume change property, the hydrogel grating immunosensors enable highly sensitive detection of H-IgG. At a fixed temperature, the value of $DE_T/DE_{T,0}$ linearly decreases with increasing the [H-IgG] value (Figure 6a), due to the h increase resulted from the H-IgG-induced swelling of hydrogel grating. For example, at T=20 °C, the $DE_T/DE_{T,0}$ value decreases from 1 to 0.77

with increasing the [H-IgG] value from 0 M to 5.3×10^{-7} M. Meanwhile, at each [H-IgG], the $DE_T/DE_{T,0}$ value decreases with decreasing temperature from 35 ºC to 20 ºC. For example, at [H-IgG]=5.3×10^{-7} M, the hydrogel grating at 35 ºC shows a $DE_T/DE_{T,0}$ value of 0.83, while the hydrogel grating at 20 ºC shows a lower $DE_T/DE_{T,0}$ value of 0.77. Such a larger decrease of $DE_T/DE_{T,0}$ value at 20 ºC indicates the a more significant volume change induced by 5.3×10^{-7} M H-IgG at 20 ºC than that at 35 ºC. The results confirm that the temperature regulation of the [H-IgG]-responsive volume change behavior of hydrogel grating based on the thermo-responsive PNIPAM backbones. Linear relationships between the R_{DE} values and the [H-IgG] values at various temperatures can be obtained quantitatively (Figure 6b), with which highly sensitive detection of H-IgG can be achieved. For example, at 20 ºC, the linear relationship between the R_{DE} value and the [H-IgG] value is quantitatively expressed as [H-IgG]=$24.636R_{DE}$ –0.0359, with correlation coefficient of 0.9974. With this equation, the [H-IgG] can be easily obtained by simply measuring the R_{DE} value of the hydrogel grating. In this study, the detection limit of [H-IgG] with our hydrogel grating immunosensors is as low as 1.3×10^{-8} M at 20 ºC. Moreover, the hydrogel grating immunosensors also allow sensitive detection of H-IgG concentration in real serum samples. By using three serum samples respectively diluted by 200 times (sample 1), 250 times (sample 2) and 300 times (sample 3) with PBS (pH=7.4, 0.1 M) for detection, the H-IgG concentration detected by the hydrogel grating immunosensor is comparable to those detected by ELISA (Table 1). The relative standard deviation (RSD) between the hydrogel grating immunosensor and ELISA are in the range from −2.42% to 5.04%, indicating good agreement between these two analytical methods. Besides, the detection performance of hydrogel grating immunosensors is comparable to other optical

immunosensors including optical fiber immunosensors and surface plasmon resonance immunosensors (Table S1), but the hydrogel grating immunosensors can provide advantages such as requirement of low-cost analytical instruments and easy operation for highly selective and sensitive H-IgG detection.

CONCLUSIONS

In summary, smart diffraction grating immunosensors based on antigen-responsive hydrogels have been developed for highly selective and sensitive detection of H-IgG. The hydrogel gratings with dual-crosslinking based on covalent bonding and dynamic antigen-antibody complexation enable enhanced H-IgG-induced swelling, which is beneficial for converting [H-IgG] signals into significant diffracted optical signals. The prepared hydrogel grating immunosensors allow highly selective and sensitive detection of [H-IgG] with detection limit as low as 1.3×10^{-8} M. Meanwhile, due to the nano-sized height of the hydrogel grating, integration of the hydrogel grating immunosensor into a portable microchip may be achieved for easy detection. Moreover, since the detection mechanism is based on the stimuli-responsive volume changes of hydrogel grating, use of other hydrogels with volume changes in response to actual disease markers such as the apple stem pitting virus,[23] detection of actual disease markers can be achieved. Thus, the strategy and results in this study provide valuable guidance for developing efficient hydrogel grating immunosensors for detection of biomarkers.

ASSOCIATED CONTENT

Supporting Information

UV analyses of washing solutions from affinity chromatography, AFM analyses of

hydrated hydrogel gratings at different temperatures, transmittance of hydrogel grating at different temperatures and comparison of performances of different optical immunosensors for detection of H-IgG. This material is available free of charge via the Internet at http://pubs.acs.org.

AUTHOR INFORMATION

Corresponding Authors

*E-mail: chuly@scu.edu.cn (L.-Y.C.).

*E-mail: wangwei512@scu.edu.cn (W.W.).

Author Contributions

The manuscript was written through contributions of all authors. All authors have given approval to the final version of the manuscript.

Notes

The authors declare no competing financial interest.

ACKNOWLEDGMENTS

The authors gratefully acknowledge support from the National Natural Science Foundation of China (21576167).

REFERENCES

(1) Sawyers, C. L. The Cancer Biomarker Problem. *Nature* **2008**, 7187, 548-552.

(2) Wu, L.; Qu, X. G. Cancer Biomarker Detection: Recent Achievements and Challenges. Chem. *Soc. Rev.* **2015**, 44, 2963-2997.

(3) Rusling, J. F.; Kumar, C. V.; Gutkind, J. S.; Patel, V. Measurement of Biomarker Proteins for Point-of-Care Early Detection and Monitoring of Cancer. *Analyst*

2010, 135, 2496-2511.

(4) Zhou, L.; Mao, H. J.; Wu, C. Y.; Tang, L.; Wu, Z. H.; Sun, H.; Zhang, H. L.; Zhou H. B.; Jia, C. P.; Jin, Q. H.; Chen, X. F.; Zhao, J. L. Label-Free Graphene Biosensor Targeting Cancer Molecules Based on Non-Covalent Modification. *Biosens. Bioelectron.* **2017**, 87, 701-707.

(5) Eriksson, C.; Kokkonen, H.; Johansson, M.; Hallmans, G.; Wadell, G.; Rantapää-Dahlqvist, S. Autoantibodies Predate the Onset of Systemic Lupus Erythematosus in Northern Sweden. *Arthritis Res. Ther.* **2011**, 13, R30.

(6) Conrad, K.; Roggenbuck, D.; Reinhold, D.; Dörner, T. Profiling of Rheumatoid Arthritis Associated Autoantibodies. *Autoimmun. Rev.* **2010**, 9, 431-435.

(7) Gonzalez-Quintela, A.; Alende, R.; Gude, F.; Campos, J.; Rey, J.; Meijide, L. M.; Fernandez-Merino, C.; Vidal, C. Serum Levels of Immunoglobulins (IgG, IgA, IgM) in a General Adult Population and Their Relationship with Alcohol Consumption, Smoking and Common Metabolic Abnormalities. *Clin. Exp. Immunol.* **2008**, 151, 42-50.

(8) Ipp, H.; Zemlin, A. E.; Glashoff, R. H.; van Wyk, J.; Vanker, N.; Reid, T.; Bekker, L. G. Serum Adenosine Deaminase and Total Immunoglobulin G Correlate with Markers of Immune Activation and Inversely with CD4 Counts in Asymptomatic, Treatment-Naive HIV Infection. *J. Clin. Immunol.* **2013**, 33, 605-612.

(9) Crivellari, F.; Mavrogiannis, N.; Gagnon, Z. Nanoparticle-Based Biosensing Using Interfacial Electrokinetic Transduction. Sensor. *Actuat. B-Chem.* **2017**, 240, 926-933.

(10) Li, R.; Wu, K.; Liu, C.; Huang, Y.; Wang, Y.; Fang, H.; Zhang, H.; Li, C. 4-Amino-1-(3-Mercapto-Propyl)-Pyridine Hexafluorophosphate Ionic Liquid

Functionalized Gold Nanoparticles for IgG Immunosensing Enhancement. *Anal. Chem.* **2014**, 86, 5300-5307.

(11) Su, X.; Chew, F. T.; Li, S. F. Design and Application of Piezoelectric Quartz Crystal-Based Immunoassay. *Anal. Sci.* **2000**, 16, 107-114.

(12) Jaruwongrungsee, K.; Waiwijit, U.; Wisitsoraat, A.; Sangworasil, M.; Pintavirooj, C.; Tuantranont, A. Real-Time Multianalyte Biosensors Based on Interference-Free Multichannel Monolithic Quartz Crystal Microbalance. *Biosens. Bioelectron.* **2015**, 67, 576-581.

(13) Qiu, G.; Ng, S. P.; Wu, C. M. L. Bimetallic Au-Ag Alloy Nanoislands for Highly Sensitive Localized Surface Plasmon Resonance Biosensing. *Sensor. Actuat. B-Chem.* **2018**, 265, 459-467.

(14) Wang, Q.; Wang, B. T. Surface Plasmon Resonance Biosensor Based on Graphene Oxide/Silver Coated Polymer Cladding Silica Fiber. *Sensor. Actuat. B-Chem.* **2018**, 275, 332-338.

(15) Zhang, D.; Gao, B.; Chen, Y.; Liu, H. Converting Colour to Length Based on the Coffee-Ring Effect for Quantitative Immunoassays Using A Ruler as Readout. *Lab Chip* **2018**, 18, 271-275.

(16) Cho, B.; Kim, S.; Woo, H. G.; Kim, S.; Sohn, H. Detection of Human Ig G Using Photoluminescent Porous Silicon Interferometer. *J. Nanosci. Nanotechnol.* **2015**, 15, 1083-1087.

(17) Lee, J.; Icoz, K.; Roberts, A.; Ellington, A. D.; Savran, C. A. Diffractometric Detection of Proteins Using Microbead-Based Rolling Circle Amplification. *Anal. Chem.* **2009**, 82, 197-202.

(18) Kaufmann, T.; Ravoo, B. J. Stamps, Inks and Substrates: Polymers in Microcontact Printing. *Polym. Chem.* **2010**, 1, 371-387.

(19) Wendeln, C.; Ravoo, B. J. Surface Patterning by Microcontact Chemistry. *Langmuir* **2012**, 28, 5527-5538.

(20) Gatterdam, V.; Frutiger, A.; Stengele, K. P.; Heindl, D.; Lübbers, T.; Vörös, J.; Fattinger, C. Focal Molography is a New Method for the In Situ Analysis of Molecular Interactions in Biological Samples. *Nat. Nanotechnol.* **2017**, 12, 1089-1095.

(21) Peng, H. Y.; Wang, W.; Gao, F.; Lin, S.; Liu, L. Y.; Pu, X. Q.; Liu, Z.; Ju, X. J.; Xie, R.; Chu, L. Y. Ultrasensitive Diffraction Gratings Based on Smart Hydrogels for Highly Selective and Rapid Detection of Trace Heavy Metal Ions. *J. Mater. Chem. C* **2018**, 6, 11356-11367.

(22) Peng, H. Y.; Wang, W.; Gao, F.; Lin, S.; Ju, X. J.; Xie, R.; Liu, Z.; Faraj Y.; Chu, L. Y. Smart Hydrogel Gratings for Sensitive, Facile, and Rapid Detection of Ethanol Concentration. *Ind. Eng. Chem. Res.* **2019**, 58, 17833-17841.

(23) Bai, W.; Spivak, D. A. A Double-Imprinted Diffraction-Grating Sensor Based on a Virus-Responsive Super-Aptamer Hydrogel Derived from an Impure Extract. *Angew. Chem. Int. Ed.* **2014**, 53, 2095-2098.

(24) Hong, Y. S.; Kim, J.; Sung, H. K. Characterization of a Functional Hydrogel Layer on a Silicon-Based Grating Waveguide for a Biochemical Sensor. *Sensors* **2016**, 16, 914-923.

(25) Barrios, C. A.; Zhen H. C.; Navarro-Villoslada, F.; López-Romero, D.; Moreno-Bondi, M. C. Molecularly Imprinted Polymer Diffraction Grating as Label-Free Optical Bio(mimetic) Sensor. *Biosens. Bioelectron.* **2011**, 26, 2801-2804.

(26) Avella-Oliver, M.; Ferrando, V.; Monsoriu, J. A.; Puchades, R.; Maquieira, A. A Label-Free Diffraction-Based Sensing Displacement Immunosensor to

Quantify Low Molecular Weight Organic Compounds. *Anal. Chim. Acta* **2018**, 1033, 173-179.

(27) Wang, X. Q.; Liu, X. Y.; Wang, X. G. Surface-Relief-Gratings Based on Molecularly Imprinted Polymer for 2, 4-dichlorophenoxyacetic Acid Detection. *Sens. Actuators, B* **2015**, 220, 873-879.

(28) Oliveira, N. C.; El Khoury, G.; Versnel, J. M.; Moghaddam, G. K.; Leite, L. S.; Lima-Filho, J. L.; Lowe, C. R. A Holographic Sensor Based on a Biomimetic Affinity Ligand for the Detection of Cocaine. *Sens. Actuators, B* **2018**, 270, 216-222.

(29) Bailey, R. C.; Nam, J. M.; Mirkin, C. A.; Hupp, J. T. Real-Time Multicolor DNA Detection with Chemoresponsive Diffraction Gratings and Nanoparticle Probes. *J. Am. Chem. Soc.* **2003**, 125, 13541-13547.

(30) Chen, J. K.; Zhou, G. Y.; Chang, C. J.; Lee, A. W.; Chang, F. C. Label-Free DNA Detection Using Two-Dimensional Periodic Relief Grating as a Visualized Platform for Diagnosis of Breast Cancer Recurrence after Surgery. *Biosens. Bioelectron.* **2014**, 54, 35-41.

(31) Gnanaprakasa, T. J.; Oyarzabal, O. A.; Olsen, E. V.; Pedrosa, V. A.; Simonian, A. L. Tethered DNA Scaffolds on Optical Sensor Platforms for Detection of hipO Gene from Campylobacter jejuni. *Sens. Actuators, B* **2011**, 156, 304-311.

(32) Acharya, G.; Chang, C. L.; Holland, D. P.; Thompson, D. H.; Savran, C. A. Rapid Detection of S-Adenosyl Homocysteine Using Self-Assembled Optical Diffraction Gratings. *Angew. Chem. Int. Ed.* **2008**, 47, 1051-1053.

(33) Avella-Oliver, M.; Carrascosa, J.; Puchades, R.; Maquieira, Á. Diffractive Protein Gratings as Optically Active Transducers for High-Throughput Label-Free Immunosensing. *Anal. Chem.* **2017**, 89, 9002-9008.

(34) Sancho-Fornes, G.; Avella-Oliver, M.; Carrascosa, J.; Morais, S.; Puchades, R.; Maquieira, Á. Enhancing the Sensitivity in Optical Biosensing by Striped Arrays and Frequency-Domain Analysis. *Sens. Actuators, B* **2019**, 281, 432-438.

(35) Chang, C. L.; Acharya, G.; Savran, C. A. In Situ Assembled Diffraction Grating for Biomolecular Detection. *Appl. Phys. Lett.* **2007**, 90, 233901.

(36) Gupta, R.; Sagade, A. A.; Kulkarni, G. U. A Low Cost Optical Hydrogen Sensing Device Using Nanocrystalline Pd Grating. *Int. J. Hydrogen Energy* **2012**, 37, 9443-9449.

(37) Bailey, R. C.; Hupp, J. T. Large-Scale Resonance Amplification of Optical Sensing of Volatile Compounds with Chemoresponsive Visible-Region Diffraction Gratings. *J. Am. Chem. Soc.* **2002**, 124, 6767-6774.

(38) Ye, G.; Yang, C.; Wang, X. G. Sensing Diffraction Gratings of Antigen-Responsive Hydrogel for Human Immunoglobulin-G Detection. *Macromol. Rapid Commun.* **2010**, 31, 1332-1336.

(39) Zhao, Y.; Ju, X. J.; Zhang, L. P.; Wang, W.; Faraj, Y.; Zou, L. B.; Xie, R.; Liu, Z.; Chu, L. Y. Transparent Thermo-Responsive Poly(*N*-isopropylacrylamide)-l-poly(ethylene glycol)-acrylamide Conetwork Hydrogels with Rapid Deswelling Response. *New J. Chem.* **2019**, 43, 9507-9515.

(40) Seo, J. H.; Chen, L. J.; Verkhoturov, S. V.; Schweikert, E. A.; Revzin, A. The Use of Glass Substrates with Bi-functional Silanes for Designing Micropatterned Cell-Secreted Cytokine Immunoassays. *Biomaterials* **2011**, 32, 5478-5488.

(41) Chen, Y.; Kang, E. T.; Neoh, K. G.; Huang, W. Electroless Metallization of Glass Surfaces Functionalized by Silanization and Graft Polymerization of Aniline. *Langmuir* **2001**, 17, 7425-7432.

(42) Miyata, T.; Asami, N.; Uragami, T. A Reversibly Antigen-Responsive Hydrogel. *Nature* **1999**, 399, 766-768.

(43) Lin S.; Wang W.; Ju X. J.; Xie R.; Liu Z.; Yu H. R.; Zhang C.; Chu L. Y. Ultrasensitive Microchip Based on Smart Microgel for Real-Time on-Line Detection of Trace Threat Analytes. *Proc. Natl. Acad. Sci. U. S. A.* **2016**, 113, 2023-2028.

(44) Yan P. J.; He F.; Wang W.; Zhang S. Y.; Zhang L.; Li M.; Liu Z.; Ju X. J.; Xie R.; Chu L. Y. Novel Membrane Detector Based on Smart Nanogels for Ultrasensitive Detection of Trace Threat Substances. *ACS Appl. Mater. Interfaces* **2018**, 10, 36425-36434.

(45) Kayaman, N.; Kazan, D.; Erarslan, A.; Okay, O.; Baysal, B. M. Structure and Protein Separation Efficiency of Poly (N-isopropylacrylamide) Gels: Effect of Synthesis Conditions. *J. Appl. Polym. Sci.* **1998**, 67, 805-814.

(46) Nayak, S.; Debord, S. B.; Lyon, L. A. Investigations into the Deswelling Dynamics and Thermodynamics of Thermoresponsive Microgel Composite Films. *Langmuir* **2003**, 19, 7374-7379.

Figures

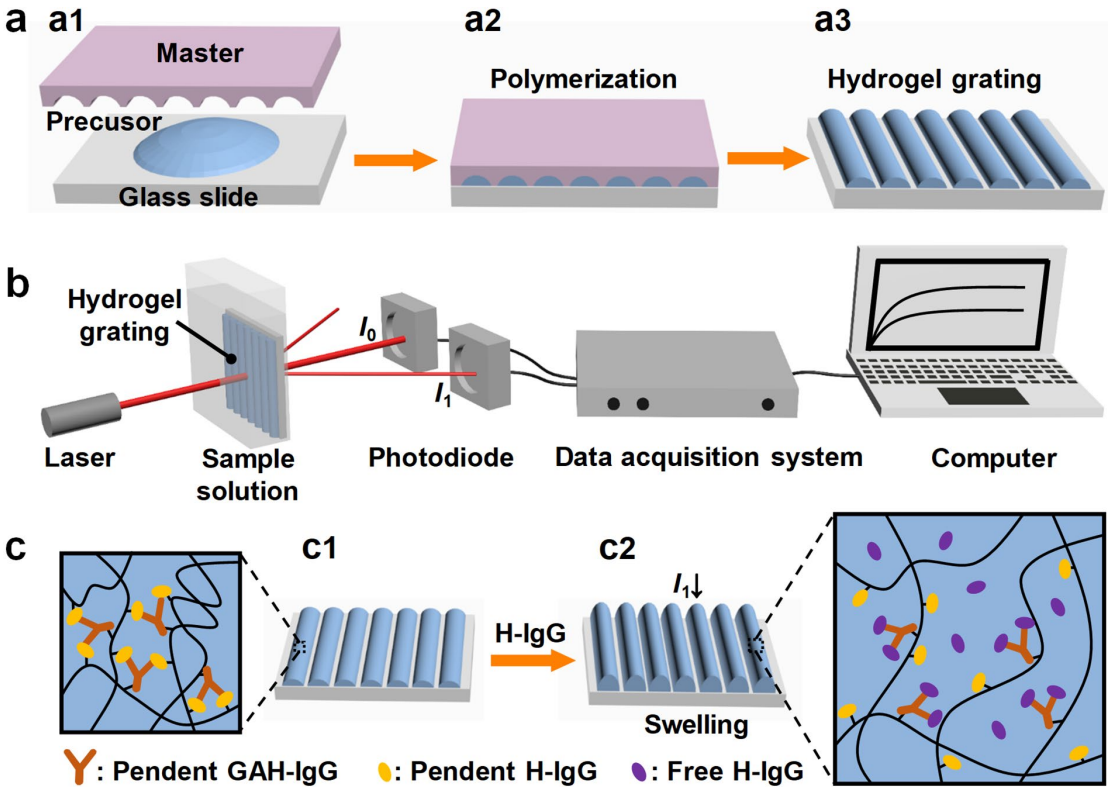

Figure 1. (a) Schematic illustration of the fabrication process of hydrogel grating by polymerization of the precursor solution templated by a stamp (a1-a2) to create the hydrogel grating on glass slide (a3). (b) Setup of the optical detection platform based on the hydrogel grating. (c) Schematic illustration of the mechanism for detection of H-IgG. The GAH-IgG/H-IgG complexes in hydrogel grating (c1) can decompose upon recognizing free H-IgG by the pendent GAH-IgG (c2), to induce a volume swelling and change of diffracted optical signal (c2).

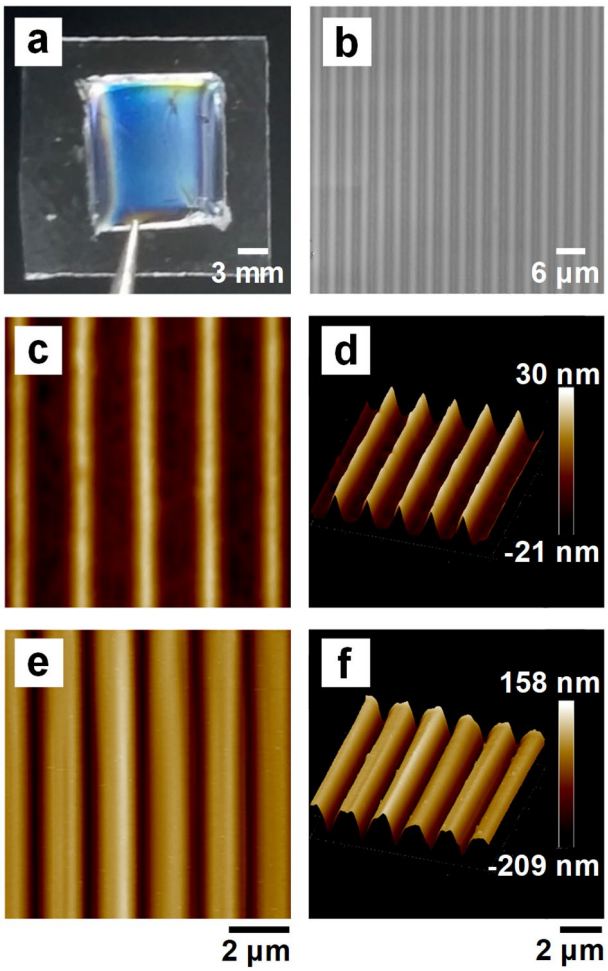

Figure 2. Morphological characterizations of antigen-responsive hydrogel gratings. (a,b) The optical (a) and SEM (b) images of the hydrogel grating. (c-f) Two-dimensional (c, e) and three-dimensional (d, f) AFM analyses of the dehydrated (c,d) and hydrated (e,f) hydrogel gratings.

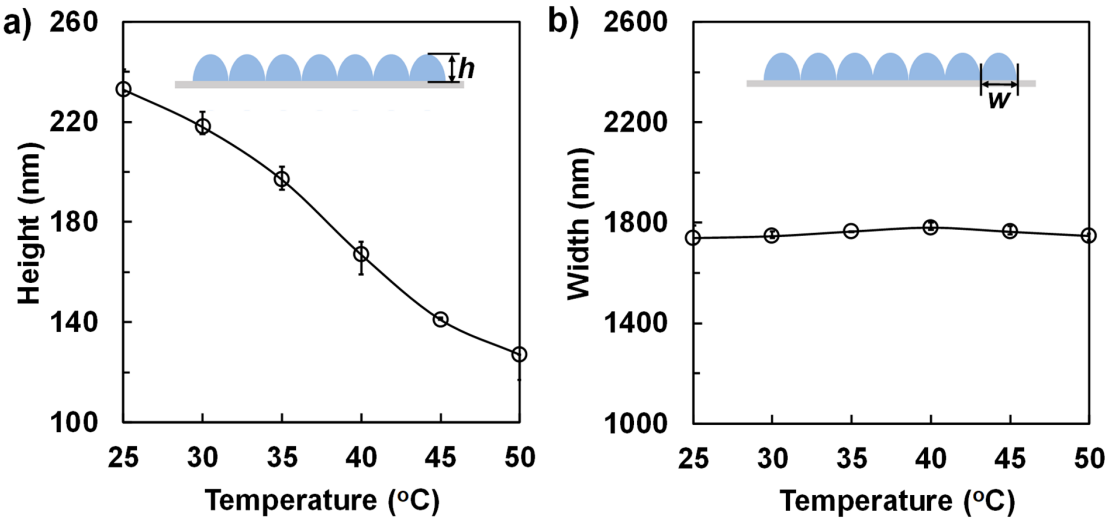

Figure 3. Temperature-dependent changes of the height (*h*) (a) and width (*w*) (b) of antigen-responsive hydrogel grating.

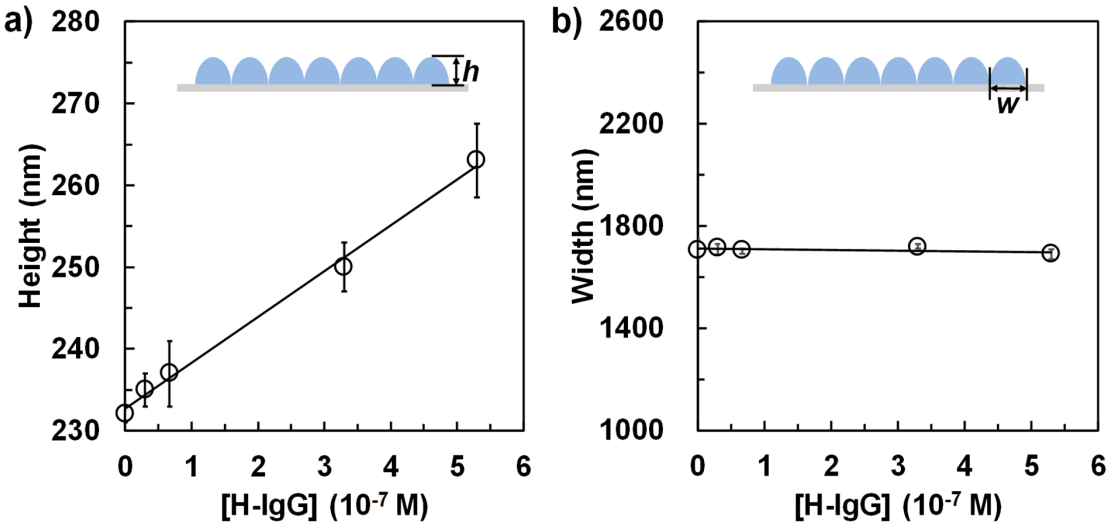

Figure 4. [H-IgG]-responsive changes of the height (*h*) (a) and width (*w*) (b) of antigen-responsive hydrogel grating at 25 ºC

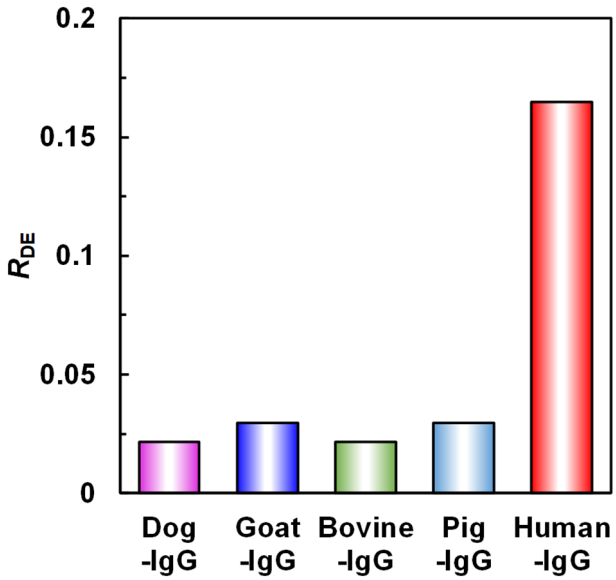

Figure 5. Highly selective detection of H-IgG. Five sample solutions respectively containing dog-IgG, goat-IgG, bovine-IgG, pig-IgG and human-IgG, each with concentration of 4×10^{-7} M, are detected at $T = 25$ °C.

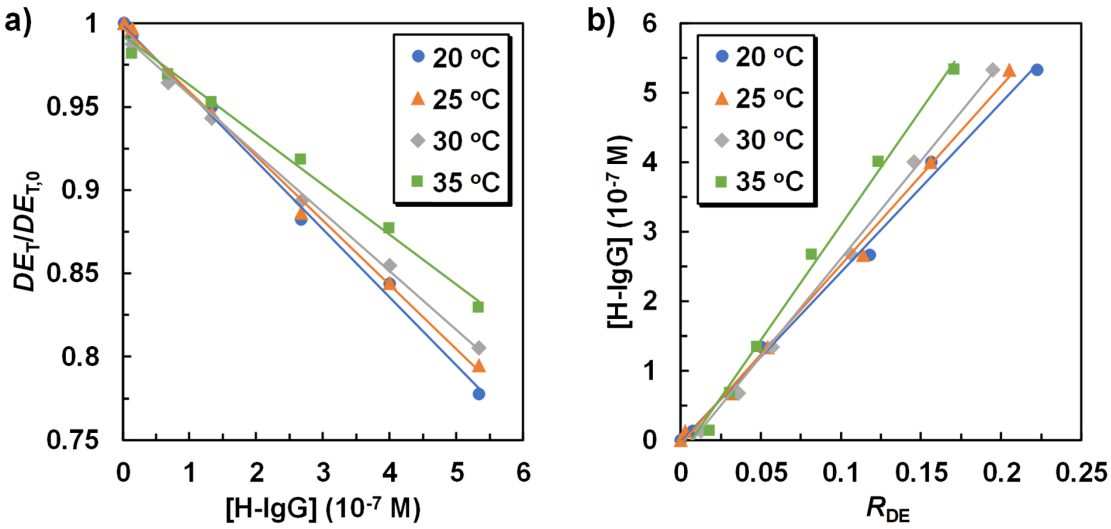

Figure 6. Highly sensitive detection of H-IgG. (a) [H-IgG]-dependent changes of $DE_T/DE_{T,0}$ at different temperatures. (b) Relationship between [H-IgG] and R_{DE} at different temperatures.

Table 1 Comparison of ELISA and the hydrogel grating immunosensor for detecting H-IgG in real serum samples

Serum samples	ELISA (μg mL^{-1})	Immunosensors (μg mL^{-1})	RSD (%)
1	60.6	63.7	5.04
2	47.6	50.1	5.25
3	38.2	37.2	-2.42

Graphic for TOC